Available online at www.sciencedirect.com
ScienceDirect
International Journal of Heat and Mass Transfer 50 (2007) 2787–2794
International Journal of HEAT and MASS TRANSFER
www.elsevier.com/locate/ijhmt

Parametric study of recuperative VOC oxidation reactor with porous media

N.N. Gnesdilov *, K.V. Dobrego, I.M. Kozlov

Heat and Mass Transfer Institute, National Academy of Sciences of Belarus, P. Brovki Street 15, Minsk 220072, Belarus

Received 9 October 2006
Available online 16 January 2007

Abstract

Numerical study of volatile organic compounds (VOC) oxidation reactor consisting of two coaxial tubes, filled with inert porous media is performed. Influence of incoming gas flux, adiabatic temperature of gas combustion, reaction rate constant, diameter of porous body particles, reactor size and heat losses on maximal temperature of reactor, recuperation efficiency, combustion front position is investigated. It is shown that maximum temperature and recuperation efficiency of reactor has extremum in the field of incoming gas flow rate and porous body particle size parameters (for simulated configuration of reactor maximum corresponds to $U_G \sim 2$ m/s and $d_0 \sim 6$ mm). Numerical simulation shows non-monotonous character of maximal temperature and recuperation efficiency dependence from side heat losses of reactor. The obtained results can be used for construction optimization of practical VOC oxidation reactors.

Keywords: Filtration combustion (FC); Heat recuperation; Heat regeneration; Porous media; Volatile organic compounds (VOC); Oxidizer

1. Introduction

Air purification from Volatile Organic Compounds (VOC) remains actual problem facing chemical, nutrition, mining and other industries [1,2]. The widely spread VOCs – phenol, formaldehyde, acetone, benzole and other may be contained in ventilation gases of mines, paint shops, plastic extruder shops, in technological flue gases, etc. In many cases VOCs concentration is less than combustion lean limit concentration, but enough for self-sustained combustion in inert porous media. Combustion in inert porous media or filtration combustion (FC) provides effective heat recirculation and consequently low energy costs of the process [3–6]. In the case of sufficiently high concentration of VOCs (~1 mass%) the combustion process may be sustained due to the heat content of the pollutants and does not demand any additional fuels. In experiments by Takeno and Sato [7] in steady reactor with complicated heat recuperation methane–air mixture combustion was realized at equivalence ratio as low as $\Phi = 0.026$ (which is 20 times lower than lean limit combustion concentration for methane–air mixture). In the work [3,4] the regenerative porous media reactor was utilized for lean methane combustion. The stable combustion was achieved at equivalence ratio $\Phi = 0.15$.

One of the principal features of FC is internal heat recirculation in the combustion wave, due to heat exchange between gas and solid in the preheat zone of the combustion wave. Practical systems designed for the low calorific fuels combustion utilize schemes of external heat recirculation in addition to the internal one. These are heat recuperation by means of counter-flow heat exchange between incoming and exhaust gases and heat regeneration due to periodical reverse of flow direction. Both schemes are investigated in laboratory installations [3,4,8–10] and found their application in industrial VOCs oxidizers, produced by Thermatrix [10], ReEco-Stroem [11] and other companies. Physical aspects of the FC in inert porous media are discussed in [4,7,12,13] and other papers.

* Corresponding author. Tel.: +375172842217; fax: +375172842212.
E-mail address: nick_gn@itmo.by (N.N. Gnesdilov).

0017-9310/$ - see front matter © 2006 Elsevier Ltd. All rights reserved.
doi:10.1016/j.ijheatmasstransfer.2006.11.004

Nomenclature

a, a_0	Arrhenius preexponential factor (m^3/(mol s))
C_r	efficiency of recuperation (dimensionless)
C_l	dimensionless losses from sidewall of reactor
c_p	heat capacity of gas (J/(kg K))
c_s	heat capacity of porous carcass (J/(kg K))
$\mathbf{D}$	gas diffusivity tensor (m^2/s)
$\mathbf{D}_d$	dispersion diffusivity tensor (m^2/s)
D_p, D_t	longitudinal and transverse component of dispersion diffusivity tensor
D_g	gas diffusivity coefficient, approximated by nitrogen properties (m^2/s)
d_0	diameter of porous carcass particle (m)
d_1	internal tube diameter (m)
d_2	reactor diameter (m)
G	gas mass flow rate (kg/s)
h_i	mass enthalpy of ith chemical component
Δh	gas mixture heat of combustion (J/kg)
$\mathbf{I}$	unit matrix
k	reaction rate (m^3/(mol s))
k_0, k_1	filtration permeabilities
M	average molecular weight of gas (kg/mol)
m	porosity
p	pressure (Pa)
p_0	outlet pressure (Pa)
Q_r	heat flux via internal tube wall (W)
Q_l	heat losses from side wall of reactor (W)
R	absolute gas constant
r	radius (m)
S	internal tube cross section (m^2)
T	temperature (K)
T_{ad}	adiabatic temperature of combustion, $\Delta T_{ad} = T_{ad} - T_0$ (K)
T_0	initial temperature of the system (K)
U_G	superficial gas velocity (m/s)
$\mathbf{u}$	gas velocity vector (m/s)
X_i	molar fraction of ith component
Y_i	mass fraction of ith component
z_1, z_2	internal tube or reactor length (m)
z_f	combustion front position (m)

Greek symbols

α	heat exchange coefficient (W/(m^2 K))
α_{vol}	volumetric heat exchange coefficient (W/(m^3 K))
ε	emissivity of the porous carcass
ρ	density (kg/m^3)
$\dot{\rho}_i$	mass generation rate of ith component due chemical reactions (kg/s)
$\boldsymbol{\Lambda}$	heat conductivity tensor (W/(m K))
λ	conductivity or effective conductivity of porous carcass (W/(m K))
μ	gas viscosity coefficient, approximated by nitrogen properties (Pa s)
σ	Stefan–Boltzmann constant (5.67×10^{-8} W/(m^2 K^4))
$\boldsymbol{\tau}$	unit vector with components τ_z, τ_r
Φ	fuel/air equivalence ratio
Ω	surface of internal tube or reactor sidewall

Subscripts

1	relates to internal tube
2	relates to reactor sidewall
g	gas
i	ith component of gas
s	solid

Though such type of reactors are under investigation and have a practical utilization, there is lack of obtainable publications concerned with detailed parametric study of these devices. The combined regenerator–recuperator scheme of VOC oxidizer was investigated in [14] numerically. Important parameters – maximal temperature of reactor, NO_x emission, effective ranges of gas flow rate and VOC concentration are compared for different types of reactor. It was shown that recuperative–regenerative scheme let one expand the range of operational flow rate and VOC concentration compared to stationary recuperative reactor.

Parametric study of filtration combustion reactor with electro heating elements was presented in [15]. The influence of gas flow rate, electrical heating elements position and power, and thermal isolation on maximal temperature in the system, unburned VOC concentration was investigated.

In this article numerical study of the steady-state recuperative (coaxial tubes type) reactor is performed. The influence of incoming gas flow rate, heat losses via side wall and other parameters on temperature and VOC burning out is under investigation. Reactor recuperation efficiency and combustion front position were under consideration too. The chemical kinetics of the VOC oxidation is modeled by one-step Brutto model for methane combustion.

2. Problem statement

The system under investigation consists of two coaxial tubes, filled with ceramic particles – packed bed (Fig. 1). The reactor walls width is assumed to be zero in the model. The heat losses via side walls may be varied according to Newtonian law (7). At initial time instant porous body (Fig. 1, (4)) was preheated in order to ignite the gas mixture. VOC containing gas (Fig. 1, (1)) enters through central tube, heats up due to the heat exchange with porous body (Fig. 1, (4)) turns-around and goes out through the gap between internal tube and reactor body (Fig. 1, (2)). At certain temperature the VOC oxidation starts and xcombustion products heat up porous media and via it the incoming fresh gas mixture.

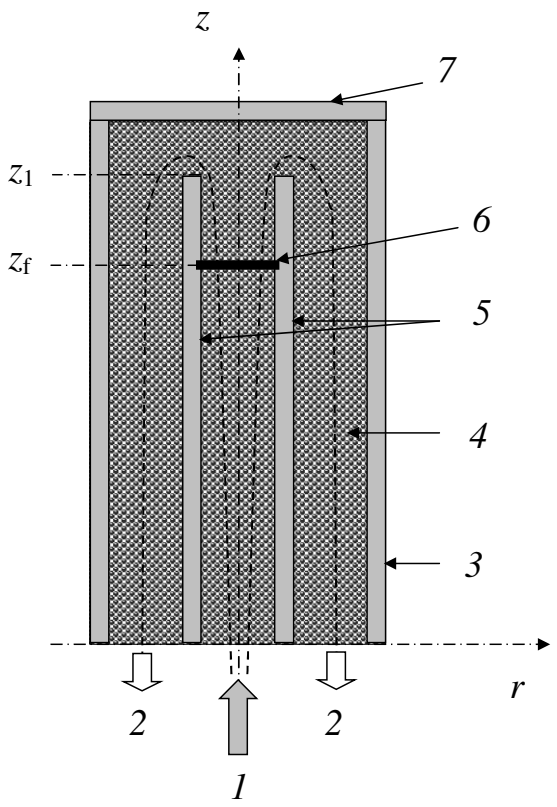

Fig. 1. Reactor scheme: (1) – incoming gases, with mass flow rate G, (2) – out coming gases, (3) – reactor side wall, (4) – porous media, (5) – internal tube, (6) – combustion front, (7) – cover, z_1 – internal tube length, z_f – combustion front position.

Investigation of the system include parametric study where the main "target" parameters defining reactors design and operation regime are maximum temperature of the porous media, recuperation efficiency, front position and VOC oxidation completeness.

3. Governing equations

Conventional volume averaged approximation was used for the system simulation [14,16,17]. The set of equations included: the continuity and filtration equations for gas, the mass conservation equation for chemical components, the thermal conductivity equations for gas and the solid phase as well as the ideal gas state equation. Gas dispersion conductivity and diffusivity are used in the diffusion and conduction Eqs. (3) and (4). Radiation conductivity is taken into consideration in the heat conductivity Eq. (5). More detailed description of the mathematical model, boundary conditions and algorithms one can find in [14,16,17].

$$\frac{\partial \rho_g}{\partial t} + \nabla(\rho_g \mathbf{u}) = 0. \tag{1}$$

$$-\nabla p = \frac{\mu}{k_0}\mathbf{u} + \frac{\rho_g}{k_1}|\mathbf{u}|\mathbf{u}. \tag{2}$$

$$\rho_g \frac{\partial Y_i}{\partial t} + \rho_g \mathbf{u}\nabla Y_i - \nabla \rho_g \mathbf{D}\nabla Y_i = \dot{\rho}_i. \tag{3}$$

$$\rho_g c_p \frac{\partial T_g}{\partial t} + c_p \rho_g \mathbf{u}\nabla T_g - \nabla \boldsymbol{\Lambda}\nabla T_g = \frac{\alpha_{vol}}{m}(T_s - T_g) - \sum_i h_i \dot{\rho}_i. \tag{4}$$

$$(1-m)\rho_s c_s \frac{\partial T_s}{\partial t} - \nabla(\lambda \nabla T_s) = \alpha_{vol}(T_g - T_s). \tag{5}$$

$$\rho_g = \frac{pM}{RT_g}. \tag{6}$$

The system (1)–(6) is added by boundary conditions for temperature, concentration and velocity. Tubes walls impermeability condition is applied for gas component concentration and velocity. Gas flow rate is fixed at the entrance cross section of the system. Constant pressure $p = p_0$ at the exit conditions is used for the filtration equation solution. Adiabatic or Newtonian condition may be applied as boundary conditions for temperature (5):

$$-\lambda \left.\frac{\partial T_s}{\partial r}\right|_{r=0.5d_2} = \alpha(T_s|_{r=0.5d_2} - T_0). \tag{7}$$

The boundary conditions are presented in more details in [17].

Dispersion diffusion and conductivity of gas are taken into the account in transport equations for a gas (3) and (4): $\mathbf{D} = D_g\mathbf{I} + \mathbf{D}_d$, where $\mathbf{D}_d = \begin{bmatrix} D_p\tau_z^2 + D_t\tau_r^2 & (D_p - D_t)\tau_z\tau_r \\ (D_p - D_t)\tau_z\tau_r & D_p\tau_r^2 + D_t\tau_z^2 \end{bmatrix}$ – dispersion diffusion tensor and $\tau = \frac{\mathbf{u}}{|\mathbf{u}|}$. Its component depends from gas velocity [18]:

$$D_p = 0.5 d_0 |\mathbf{u}|; \; D_t = 0.1 d_0 |\mathbf{u}|. \tag{8}$$

$$\boldsymbol{\Lambda} = \lambda_g \mathbf{I} + c_p \rho_g \mathbf{D}_d \tag{9}$$

is dispersion conductivity tensor.

Radiation component of porous body conductivity is taken into the account in energy balance equation according to [19]:

$$\lambda = \lambda_s + \frac{16}{3}\left(\frac{0.666m}{(1-m)}\right)\varepsilon\sigma d_0 T_s^3. \tag{10}$$

Volumetric heat exchange coefficient between gas and porous body is [20]:

$$\alpha_{vol} = \frac{\lambda_g 6(1-m)}{d_0^2}\left[2 + 1.1\left(\frac{\mu c_p}{\lambda_g}\right)^{1/3}\left(\frac{\rho_g u_g d_0}{\mu}\right)^{0.6}\right]. \tag{11}$$

The values of the system parameters in the standard case are presented in the Table 1. Diameters of tubes d_1 and d_2 were chosen in a way to give equal cross-section for incoming and outcoming gases.

VOC-containing gas was modeled by methane–air mixture with component ratio $N_2{:}O_2{:}CH_4 = 80{:}20{:}1$ (equivalence ratio $\Phi = 0.1$) in standard case. One step second order methane oxidation reaction was considered $CH_4 + 2O_2 \xrightarrow{k} CO_2 + 2H_2O$.

Oxidation rate was simulated by Arrhenius formula with the constants taken from [21]:

$$\frac{dX_{CH_4}}{dt} = -aX_{CH_4}X_{O_2}\exp(-15,640/T_g). \tag{12}$$

Table 1
Standard values of the problem parameters

Parameter	Dimension	Value	Parameter description
a	$m^3/(mol\ s)$	2.17×10^8	Preexponential factor in Arrhenius law (12)
		2.17×10^7–2.17×10^{10}	Varied
c_s	J/kg/K	1300	Porous body material heat capacity
d_0	mm	4.8	Packed bed particle diameter
		1–8	Varied
d_1	cm	2.8	Central tube diameter
		1.8–3.6	Varied
d_2	m	0.04	Reactor diameter
m	–	0.4	Porosity
p_0	Pa	1.01325×10^5	Pressure at exit of reactor
T_0	K	300	Initial temperature of the system
U_G	m/s	1.0	Gas superficial velocity
		0.1–5	Varied
z_1	m	0.37	Central tube length
z_2	m	0.4	Reactor length
α	$W/m^2/K$	0	Heat transfer coefficient between reactor side wall and ambient
		0–10	Varied
α_{vol}	$W/m^3/K$	$\sim 10^5$	Volumetric heat transfer coefficient, calculated during simulation
ε	–	0.45	Emissivity of the packed bed particles
λ_s	W/m/K	1.87	Porous body material thermal conductivity coefficient
ρ_s	kg/m^3	3987	Porous body material density
Φ	mol/mol	0.1	Fuel oxidizer equivalence ratio, corresponded $\Delta T_{ad} \approx 282.9$ K
		0.03–0.3	Varied

The 2DBurner software package was used to solve two-dimensional problem (1)–(6) [17]. Normally after 5–15 min of physical time the system came to steady state. The steady-state solution was used to generate the data for parametric study of the system.

4. Parametric study results and discussion

The most important for construction and exploitation of the VOC oxidation reactor parameters are VOC remains on exit, maximal gas and porous carcass temperatures and efficiency of heat recuperation C_r, determined as follows:

$$C_r = Q_r/\Delta hG. \tag{13}$$

Here $Q_r = \int_{\Omega_1} \lambda \frac{\partial T}{\partial r} dS$ is conductivity heat flux from combustion products to fresh incoming gas via the internal tube wall and inter phase heat exchange, Ω_i is a side wall surface of internal tube.

Combustion front position z_f at different parameters was studied because of z_f influence on recuperative heat flux Q_r and recuperation efficiency C_r. Actually, after VOC burn out in combustion front, temperature of gas does not increase downstream and in the case of adiabatic reactor remains constant until heat exchange with incoming gas starts at $z < z_f$. That is why recuperative heat flux via internal tube wall is zero at coordinate $z \geqslant z_f$ and only part of the reactor length participates in the heat recuperation from out coming gases to incoming ones.

The simulation shows insignificant difference between the maximal temperature of gas and porous carcass and, therefore, only maximal temperature of porous carcass is presented on figures below. The data of VOC burn out are not presented in the paper. In all steady-state operational regimes the unburned methane concentration was less than 10^{-6} mol/mol.

Influence of gas velocity U_g, fuel/oxidizer equivalence ratio Φ, reaction constant rate factor k, heat exchange coefficient α on maximal porous body temperature $T_{s,max}$, front position z_f and heat recuperation efficiency C_r were investigated numerically. The data obtained for different Φ were recalculated and presented as a function of $\Delta T_{ad} = \Delta h/c_p$, where heat capacity c_p of gas mixture assumed to be constant $c_p = 1025$ J/kg/K.

4.1. The influence gas velocity U_g on maximal porous body temperature $T_{s,max}$, front position z_f and recuperation efficiency C_r

The graphs in Fig. 2(a) demonstrate non-monotonous behavior of $T_{s,max}(U_G)$ and $C_r(U_G)$ functions. The maximum of both functions lay near $U_G = 2$ m/s. To investigate the physical nature of the non-monotonous behavior, we performed the simulation at reduced values of transport parameters D_p, D_τ and at $\varepsilon = 0.2$, it reduce effective diffusion and heat conductivity of gas and effective heat conductivity of porous carcass. Variation of the above parameters did not change significantly neither character of the curves nor absolute values of maximal temperature, efficiency of heat recuperation and front position.

4.2. The influence of adiabatic temperature ΔT_{ad} on maximal porous body temperature $T_{s,max}$, front position z_f and recuperation efficiency C_r

The adiabatic combustion temperature is natural characteristic of the fuel mixture heat content. Its influence

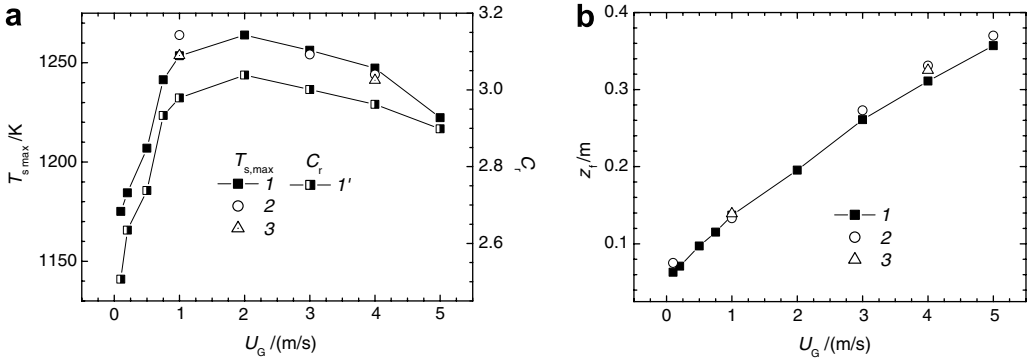

Fig. 2. Dependence of maximal temperature $T_{s,max}$, recuperation efficiency C_r – (a) and front position z_f – (b) on gas velocity U_G. 1,1′ – standard case; (2) – dispersion diffusion coefficients D_p, D_τ decreased in 2.4 times; (3) – porous body emissivity $\varepsilon = 0.2$.

on main parameters of the reactor is illustrated in Fig. 3. The graphs in Fig. 3(a) show that maximal porous body temperature $T_{s,max}$ and Q_r/z_f ratio increase nearly linearly with ΔT_{ad} increase. Combustion front shifts upstream (to inlet) as is seen from Fig. 3(b). As it was shown above, recuperation efficiency C_r correlates with front position. Simulation show that combustion is impossible in the system for very low calorific mixtures $\Delta T_{ad} \leqslant 49.4$ ($\Phi \leqslant 0.03$).

4.3. The influence of reaction rate preexponential factor (12)(a) on maximal porous body temperature $T_{s,max}$, front position z_f and recuperation efficiency C_r

Preexponential factor a characterizes reactivity of the fuel mixture. For alkanes it is not strongly varying factor, but taking in mind combustion of oxygen-, nitrogen-containing VOCs or other specific components this investigation may be of practical importance. We used dimensionless factor a/a_0 as variable in our study. Simulation (Fig. 4) show decrease of the maximal temperature $T_{s,max}$ with a growth. This "paradoxical" behavior has simple explanation. At increased reaction rate combustion processes goes faster and combustion zone shifts upstream. The consequent decrease of the front coordinate eliminate heat recuperation resulting in decrease of $T_{s,max}$. In the fast reaction limit ($a/a_0 \to \infty$) the temperature will reach the value $T_0 + \Delta T_{ad}$. The quantitative presentation of this effect is given in Fig. 4.

4.4. The influence of porous body element diameter d_0 on maximal temperature $T_{s,max}$, front position z_f and recuperation efficiency C_r

It is known that porous body particle size is important parameter defining heat and mass transfer in porous media and FC dynamics. In the steady state regime of reactor the heat recuperation efficiency C_r as well as maximal carcass temperature are also determined by d_0 (Fig. 5). For the case of the simulated system both parameters exhibit maximums at the value of $d_0 \approx 6$ mm (Fig. 5(a)). Front position is nearly linear function of d_0. The front position shift downstream with increase of d_0 (Fig. 5(a)) is explained by rather rapid decrease of the heat exchange coefficient (11). Note that normally the growth of z_f correlates with the growth of the recuperation coefficient C_r, but in the case of big elements of the porous media ($d_0 > 6$ mm) heat exchange coefficient decreases too fast and recuperation coefficient C_r falls with it. This non obvious effect deserves thorough consideration when designing practical devices.

4.5. The influence of internal tube diameter d_1 on maximal temperature $T_{s,max}$, front position z_f and recuperation efficiency C_r

To determine the influence of geometrical factors on main parameters of reactor we varied diameter of internal

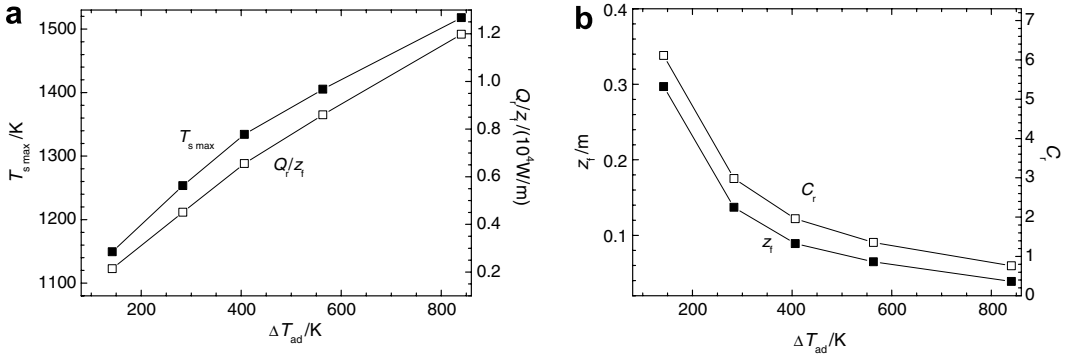

Fig. 3. Dependence of maximal temperature of porous carcass $T_{s,max}$ – (a), relationship Q_r/z_f – (a), front position z_f – (b) and recuperation efficiency coefficient C_r – (b) on ΔT_{ad}.

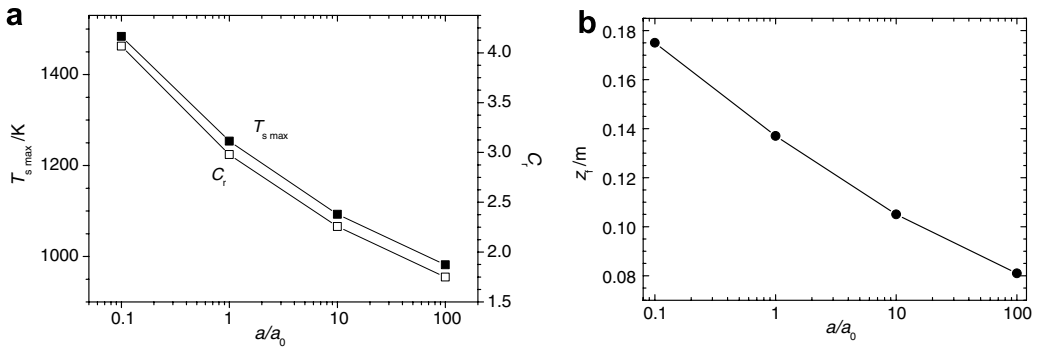

Fig. 4. Porous carcass maximal temperature $T_{s,max}$ (line 1 at (a)), recirculation heat Q_r (line 2 at (a)), and flame front position coordinate z_f – (b) dependence on preexponential factor in the Arrhenius law (12) a/a_0. Here $a_0 = 2.17 \times 10^8$ m^3/(mol s). All parameters are in SI units.

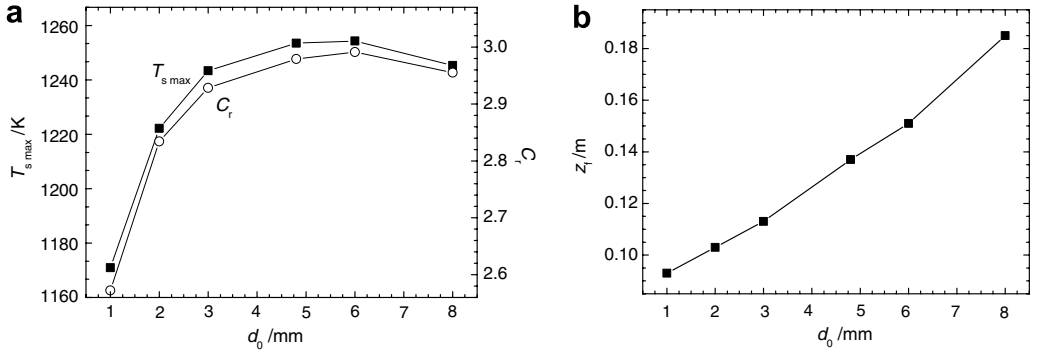

Fig. 5. Porous carcass maximal temperature $T_{s,max}$ – (a), recuperation coefficient C_r – (a) and combustion front position z_f – (b) dependence on porous bed particles diameter d_0. Here d_0 in mm other parameters in SI units.

tube, the external tube diameter being conserved. Simulation show (Fig. 6(b)) that combustion front position z_f shifts to the outlet with internal tube diameter d_1 decrease. The principal physical factor here is growth of gas flow rate and velocity. Front position shift leads to growth of recuperation heat (as discussed earlier) and consequently $T_{s,max}$. Note that with further decrease of d_1 to 1.6 cm ($d_1/d_2 = 0.4$) combustion front bowed out from internal tube and steady combustion becomes impossible. It can be seen from comparison of Fig. 6(a) and (b), that $C_r(d_1/d_2)$ and $z_f(d_1/d_2)$ functions has similar character.

4.6. The influence of heat transfer coefficient α on maximal temperature $T_{s,max}$, front position z_f, recuperation efficiency C_r and integral heat losses of reactor

Simulations were performed for the two ways of reactor feeding: 1 – gas input to the central tube and output through the gap between the tube and reactor body and 2 – reverse feeding. Non-dimensional losses from side wall of reactor was defined as $C_l = Q_l/\Delta hG$, where $Q_l = \int_{\Omega_2} \alpha(T_s - T_0)\mathrm{d}S$ is heat flux from the reactor side wall to surroundings.

Simulation shows that the front position z_f and the heat losses from the reactor side wall do not depend considerably

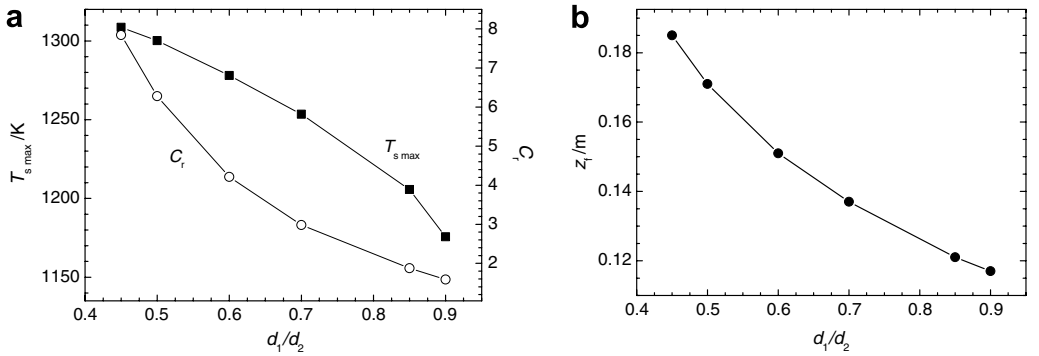

Fig. 6. Porous carcass maximal temperature $T_{s,max}$ – (a), recuperation coefficient C_r – (a) and combustion front position z_f – (b) dependence on tube diameters ratio.

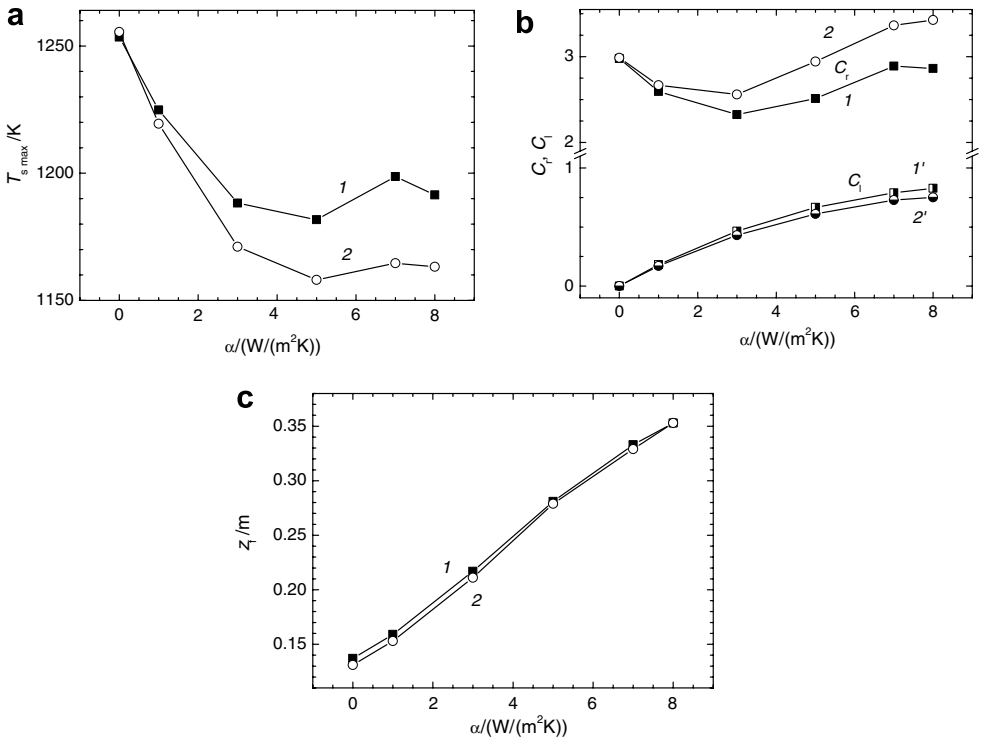

Fig. 7. Porous body maximal temperature $T_{s,max}$ – (a) recuperation efficiency, heat losses from side wall of reactor C_r – (b) and front position z_f – (c) dependence on heat transfer coefficient α. 1,1′ – gas income in the internal tube, 2,2′ – gas income in the gap between internal tube and reactor body.

on feeding way (Fig. 7(b) and (c), curves $1, 1'$ and $2, 2'$). One can see (Fig. 7(a)) the increase of $T_{s,max}$ and recuperation efficiency C_r within $\alpha = 4$–7 W/(m^2 K). This behavior is explained by the increase of the front position coordinate z_f. Actually, the heat recuperation interface is limited by $z < z_f$ area while the external heat losses C_l take place from the bigger part of the side wall of the reactor ($z_f < z < z_2$). Increasing of z_f results, from one hand, in increase of the heat recuperation area, consequently, increases Q_r and, from the other hand, decrease area of the reactor heat exchanging with environment. These two factors lead to local $T_{s,max}$ growth with α increase. When the heat exchange coefficient α reaches to 10 W/m^3 K, steady regime of combustion became impossible.

5. Conclusion

Results of detailed simulation of the recuperative steady-state VOC oxidation filtration combustion reactor was presented in this paper. The maximum temperature, combustion front position and recuperation efficiency were investigated as functions of input gas flow rate, fuel mixture heat content, reaction rate constant, intensity of external heat losses of reactor and some other parameters.

It is shown in the paper that several important parametric dependencies have a non-monotonous hardly predictable nature determining optimal constructive parameters for the given technical application of reactor. For example, maximum temperature of porous media (necessary for effective VOC oxidation), may be reached in the field of two parameters – porous body particles size and gas filtration rate. For the simulate system the optimal filtration velocity is estimated as $U_g \approx 2$ m/s. Optimal diameter of porous body particles is $d_0 = 6$ mm.

Internal tube diameter decreasing shifts front position to outlet of internal tube, increasing maximal temperature and recuperative efficiency of the reactor. From the other hand decrease of the tube diameter diminishes the operational range of gas flow rates. In the case of relatively low specific gas flow rates, reactor optimization may be performed in view of diminishing of d_1/d_2 ratio.

Two geometries of the reactor gas feed was tested numerically – feed though internal tube and contrary via external tube. In conditions of non-adiabatic reactor gas feed via internal tube is preferable.

A set of questions important for practical devices exploitation and design, namely, flame front stability problem was not touched in this paper. According to [12] the stationary filtration combustion fronts are stable to 2D thermal and hydrodynamic perturbations if the hot zone is wider than tube diameter. In the case of flame stabilization near the end of the internal tube (maximising recuperation efficiency) the question of flame stability should be revised.

Acknowledgements

The study was performed under the support of Fund for fundamental research of Republic of Belarus (Grant T05-259).

References

[1] R.J. Martin et al., Selecting the most appropriate HAP emission control technology, The Air Pollution Consultant 3 (2) (1993) 1.1–1.9.

[2] Yu.S. Matros, A.S. Noskov, V.A. Chumachenko, Catalytic recreation of industrial flue gases. Nayka Publ., Novosibirsk, 1991, pp. 22–37 (in Russian).

[3] F. Contarin, A.V. Saveliev, A.A. Fridman, L.A. Kennedy, Int. J. Heat Mass Transfer 46 (2003) 949–961.

[4] L.A. Kennedy, A.A. Fridman, A.V. Saveliev, Superadiabatic combustion in porous media: wave propagation, instabilities, new type of chemical reactor, Int. J. Fluid Mech. Res. 22 (1995) 1–26.

[5] J.G. Hoffman, R. Echigo, H. Yoshida, S. Tada, Experimental study on combustion in a porous media with a reciprocating flow system, Combust. Flame 111 (1997) 32–46.

[6] W.D. Binder, R.J. Martin, The Destruction of Air Toxic Emissions by Flameless Thermal Oxidation, Presented at 1993 Incineration Conf., Knoxville, Tennessee, 4 May, 1993.

[7] T. Takeno, K. Sato, An analytical study on excess enthalpy flames, Combust. Sci. Technol. 20 (1979) 73.

[8] M.K. Drayton, A.V. Saveliev, L.A. Kennedy, A.A. Fridman, Y.E. Li, Superadiabatic partial oxidation of methane in reciprocal and counterflow porous burners, in: Proc. of The 27th Symp. Int. on Combust. Pittsburg, PA. 1998, pp. 1361–1367.

[9] A.N. Migoun, A.P. Chernukho, S.A. Zhdanok, Numerical modeling of reverse-flow catalytic reactor for methane partial oxidation, in: Proc. of the Non-equilibrium processes and their applications, V Int. School-seminar. Minsk 2000, pp. 131–135.

[10] Available from: <http://www.thermatrix.com/>.

[11] Available from: <http://www.eco-web.com/>.

[12] K.V. Dobrego, S.A. Zhdanok (in Russian), in: Physics of filtration combustion of gases, HMTI Publishers, Minsk, 2002.

[13] K. Hanamura, R. Echigo, S. Zhdanok, Superadiabatic combustion in a porous medium, Int. J. Heat Mass Transfer 36 (13) (1993) 3201–3209.

[14] K.V. Dobrego, N.N. Gnesdilov, I.M. Kozlov, V.I. Bubnovich, H.A. Gonzalez, Numerical investigation of the new regenerator–recuperator scheme of VOC oxidizer, Int. J. Heat Mass Transfer 48 (2005) 4695–4703.

[15] N.N. Gnesdilov, K.V. Dobrego, I.M. Kozlov, E.S. Shmelev, Numerical study and optimization of the porous media VOC oxidizer with electric heating elements, Int. J. Heat Mass Transfer 49 (2006) 5062–5069.

[16] K.V. Dobrego, I.M. Kozlov, S.A. Zhdanok, N.N. Gnesdilov, Modeling of diffusion filtration combustion radiative burner, Int. J. Heat Mass Transfer 44 (2001) 3265–3272.

[17] Dobrego K.V., Kozlov I.M., Gnesdilov N.N., Vasiliev V.V., 2DBurner – software package for gas filtration combustion systems simulation and gas non-steady flames simulation, Heat and Mass Transfer Institute. Minsk 2004. Preprint N1.

[18] N. Wakao, S. Kaguei, Heat and mass transfer in a packed beds, Gordon and Breach, New York, 1982.

[19] O.E. Gorelik, V.V. Levdansky, V.G. Leitsina, N.V. Pavlyukevich, On radiation absorption in a high-porous material layer, J. Eng. Phys. Thermophys. 50 (1986) 999–1004.

[20] M. Kaviani, Principles of Heat Transfer in Porous Media, Springer-Verlag, New York, Berlin, Heidelberg, 1995.

[21] V.Ya. Basevich, A.A. Belyaev, S.M. Frolov, "Global" kinetic mechanism for turbulent reacting flow modeling. Part 1. Main chemical process of heat release, Chem. Phys. 17 (9) (1998) 117–129 (in Russian). M. Nauka.